Permeation selectivity in the electro-dialysis of mono- and divalent cations using supported liquid membranes

Qian, Zexin; Miedema, Henk; de Smet, Louis C.P.M.; Sudhölter, Ernst J.R.

DOI
10.1016/j.desal.2021.115398

Publication date
2022

Document Version
Final published version

Published in
Desalination

Desalination 521 (2022) 115398

Contents lists available at ScienceDirect

Desalination

journal homepage: www.elsevier.com/locate/desal

Permeation selectivity in the electro-dialysis of mono- and divalent cations using supported liquid membranes

Zexin Qian [a,b,*], Henk Miedema [b,**], Louis C.P.M. de Smet [b,c], Ernst J.R. Sudhölter [a,d]

[a] Department of Chemical Engineering, Delft University of Technology, Van der Maasweg 9, 2629 HZ Delft, the Netherlands
[b] Wetsus, European Centre of Excellence for Sustainable Water Technology, Oostergoweg 9, 8911 MA Leeuwarden, the Netherlands
[c] Laboratory of Organic Chemistry, Wageningen University, Stippeneng 4, 6708 WE Wageningen, the Netherlands
[d] University of Twente, Membrane Science and Technology, P.O. Box 217, 7500 AE Enschede, the Netherlands

HIGHLIGHTS

- First-time, monovalent/divalent ion-selective electro-dialysis with a supported liquid membrane (SLM)
- Ion permeation selectivity: $K^+ > Na^+ > Ca^{2+} > Mg^{2+}$
- Electrophoretic mobility: dehydrated ions ($Na^+ > K^+$) > partly hydrated ions ($Mg^{2+} > Ca^{2+}$ ions)
- Ion-exchange selectivity constant between water and membrane: $K^+ > Ca^{2+} > Mg^{2+} \approx Na^+$
- Observed permeation selectivities determined by balance of ion-exchange selectivity and electrophoretic mobilities.

ARTICLE INFO

Keywords:
Supported liquid membrane
Electro-dialysis
Ion selectivity
Ion exchange
Ion electro-phoretic mobility
Ion dehydration

ABSTRACT

We investigated in detail the permeation selectivity in the electro-dialysis of Na^+, K^+, Mg^{2+} and Ca^{2+} in both binary and quaternary mixtures using a supported liquid membrane (SLM). The SLM consisted of the organic liquid 2-nitrophenyl octyl ether (NPOE) containing a lipophilic anion, *i.e.* tetrakis[3,5-bis(trifluoromethyl) phenyl]borate, as the cation-exchanging site, which was used to fill the pores of the supporting membrane Accurel^R. We first determined the electro-phoretic mobilities of the migrating cations in single salt solutions, yielding: $Na^+ > K^+ > Mg^{2+} > Ca^{2+}$. This order reflects the different size of the migrating cations. The monovalent cations Na^+ and K^+ migrate in the dehydrated state and the divalent cations Ca^{2+} and Mg^{2+} migrate in a (partly) hydrated state, a conclusion was supported by Karl Fisher titrations.

Both binary and quaternary salt experiments showed a permeation selectivity in the following order: $K^+ > Na^+ > Ca^{2+} > Mg^{2+}$. Since this order does not correlate with the order of electro-phoretic mobilities, we have determined the ion-exchange selectivity constant (K_{ex}) and found: $K^+ > Ca^{2+} > Mg^{2+} \approx Na^+$. We conclude that the overall permeation selectivity is determined by the combination of ion-exchange selectivity and electro-phoretic mobility of the cations present in the membrane.

1. Introduction

Electrodialysis (ED) is a mature electrochemical separation process that has been applied to wastewater treatment and to the production of clean water for more than 70 years [1]. For certain applications with specific requirements for ion separation, water and ion recovery or for operation under harsh conditions, ED has become one of the state-of-art technologies [2,3]. In ED an applied electrical field is used to enhance the transport of ions from one solution through ion-exchange membranes (IEMs) into another solution, making it possible to separate a salt stream into desalinated water and brine. IEMs are the core components in such a separation process as they are permselective for cations or anions *via* ion-exchange sites that carry the opposite charge. However, the lack of selectivity between ions carrying the same charge still limits their use in separation processes where such selectivity is crucial [4,5]. In various practical applications, including fuel cells, resource recovery

* Correspondence to: Z. Qian, Department of Chemical Engineering, Delft University of Technology, Van der Maasweg 9, 2629 HZ Delft, the Netherlands.
** Corresponding author.
E-mail addresses: zexin.qian@hotmail.com (Z. Qian), henk.miedema@wetsus.nl (H. Miedema).

https://doi.org/10.1016/j.desal.2021.115398
Received 17 July 2021; Received in revised form 11 October 2021; Accepted 13 October 2021
Available online 22 October 2021

using ED and electro-membrane based batteries [6–10], the development of IEMs having excellent ion selectivity between monovalent and multivalent ions (*e.g.* Li^+/Mg^{2+}, Cl^-/SO_4^{2-}) or between ions with same valence (Cl^-/NO_3^-, Na^+/K^+) is urgently desirable [11].

In general, the widely reported selectivities for specific ions by an IEM can be summarised in four categories: (1) tailor the permeation selectivities of the ions carrying the same charge on the basis of their mobility in the membrane matrix (*e.g.*, by their ion size and the structure of the membrane including pore size and porosity) [12], (2) the observed rejection of certain ions by surface modification of the IEM using a thin polyelectrolyte layer carrying a charge opposite to the charge of the IEM [13] or the build-up of a polyelectrolyte multilayer [14,15], and (3) the observed specific interactions of the ions to be separated with added functionalities present in the IEM [16,17] or in an added coating [18]. (4) A final category is based on recent research results [19,20] that points to the role of ion dehydration in the selective transport in IEMs. The use of selective IEMs for the separation of monovalent from divalent or multivalent ions has been reported [21–25]. Most widely used commercially available Neosepta, Fuji and Nafion cation ion membranes (CEMs) have a monovalent or monovalent over divalent cation selectivity ranging from 0.5–2 [26,27]. In general, surface modification of standard CEMs improves the membrane cation selectivity [28]. Yang et al. [17], reported that surface modification of the sulfonated polysulfone (SPSF) CEMs with crown ether improve the membrane K^+/Li^+ and K^+/Mg^{2+} selectivity to 3- and 6-fold, respectively. By the adsorption of polyelectrolyte multilayers on the Nafion membrane, Zhu et al. [26] reported an improved K^+/Mg^{2+} and Li^+/Co^{2+} selectivity by a factor 1000. However, it is still currently highly challenging to separate selectively two ions that have the same valence and have similar chemical properties, *i.e.* the separation of monovalent (K^+/Na^+) or divalent cations (Ca^{2+}/Mg^{2+}).

Previous studies from our lab were focused on the separation of alkali metal cations (especially K^+ from Na^+) using a supported liquid membrane (SLM) under ED conditions and its application in the field of element recovery, stimulated by the urgent need in the context of more severe legislation of salt discharges in the greenhouse industry [20,29]. In short, an SLM is made by filling the pores of an inert porous supporting membrane with an organic solvent containing a lipophilic salt to introduce the desired permselectivity [30,31]. The lipophilic salt also contributes to a reduction of the membrane electrical resistance [32–34]. In our earlier study we investigated cation-exchange membranes (CEMs), made by the introduction of lipophilic borate anions in the immobilized organic solvent (here, 2-nitrophenyl octyl ether, NPOE), and observed the selective permeation of K^+ relative to Na^+ and Li^+ [20]. The observed permeation selectivity of $K^+ > Na^+ > Li^+$ is in line with the order of increasing dehydration energy, *i.e.* $K^+ < Na^+ < Li^+$. The measured electrophoretic ion mobility increased in the order of $K^+ < Na^+ < Li^+$, implying that the smallest ion (Li^+) moves the fastest in the membrane. Overall, we concluded that despite the higher electrophoretic mobility of the Li^+ ion, the permeability of the K^+ is the highest because of the highest exchange selectivity, which, in turn, results from its low dehydration energy. The permeation selectivity is thus dominated by the dehydration energy of the ion species present.

The current study investigates the permeation selectivity for K^+ in relation to Ca^{2+} and Mg^{2+}, as well as the permeation selectivity for Ca^{2+} in relation to Mg^{2+}. Interpretation of the obtained results includes the electrophoretic mobility of the investigated ions through the membrane, the extent of hydration of the exchanged cations and the ion-exchange selectivity at the water-membrane interface.

2. Materials and methods

2.1. Chemicals

All chemicals used were of analytical grade and used as received. The ACCUREL membrane support (polypropylene, thickness: 100 μm, pore size (diameter): 0.1 μm) was purchased from MEMBRANA, the organic solvent 2-nitrophenyl-n-octyl ether (NPOE) and the lipophilic anion A: sodium tetrakis[3,5-bis(trifluoromethyl)phenyl]borate (NaBArF) for preparing the SLM were both purchased from Sigma-Aldrich. All salts for making the salt solutions (KCl, NaCl, $CaCl_2$, $MgCl_2$ and Na_2SO_4) were purchased from MERCK.

2.2. Membrane preparation

All experiments were performed with freshly prepared SLMs. The membrane support (ACCUREL) was cut into proper shape and, without any further pretreatment, submerged in the organic solution of 50 mM NaBArF in NPOE for 30 min at room temperature. Due to capillary forces, the ACCUREL pores are filled up with the solution. Before mounting the membrane in an ED cell (Section 2.3.1), excess of solvent was removed by gently wiping it with a tissue.

2.3. Membrane characterization

2.3.1. Electrodialysis (ED)

All studies regarding ion transport across the SLMs were performed under ED conditions. Experiments were carried out in a six-compartment cell that has been reported in our previous study with the configuration shown in Fig. 1 [20]. The membrane surface area and thickness of the SLMs were 10.15 cm^2 and 100 μm, respectively with a porosity $\Phi = 0.7$ and a tortuosity $\tau = 2.1$ (membrane property data are obtained from the manufacture and literature) [35,36]. The mixed-salt experiments were carried out in equimolar 25 mM solutions of NaCl, KCl, $CaCl_2$ and $MgCl_2$ or in equimolar 50 mM binary ion solutions of KCl + $CaCl_2$, KCl + $MgCl_2$ or $CaCl_2$ + $MgCl_2$. The single-salt experiments were carried out using 0.1 M NaCl, KCl, $CaCl_2$ and $MgCl_2$ solutions. The buffer and electrolyte solutions were made with NaCl and Na_2SO_4 solutions, respectively, that have the same ionic strength as the testing solution. The testing solutions were all recirculated at a flow rate of 150 mL min^{-1} separately as feed and receiving phase in compartments A and B (Fig. 1). Prior to use, SLMs were pre-conditioned for 24 h in the solution with the same ion composition and concentration as the test solution. Commercially available standard grade cation exchange membranes (CEMs) and anion exchange membranes (AEMs) from Neosepta were used in the six-compartment cell and pre-conditioned in the same way as the SLM. The temperature of all solutions was controlled at 25 ± 0.2 °C during the experiment using a water bath. A potentiostat (Ivium Technologies, Vertex.One, Eindhoven, the Netherlands) was employed as power source for applying a constant current density. The presence of diffusion boundary layers at the membrane-solution interface can contribute to the total measured resistance. In order to minimize this effect, two Haber-Luggin capillaries were positioned directly adjacent (as close as possible) to the SLM surface and connected to two reservoirs containing 3 M KCl filled Ag/AgCl reference electrodes (QM711X, QIS, the Netherlands) for monitoring the voltage drop over the membrane. For all ED experiments, a constant current of 10 mA (corresponding to a current density of 10 A·m^{-2}) was applied during a time-period of 24 h (for single-salt experiments) or 48 h (for all mixed-salt experiments).

2.3.2. Transport numbers and mobility

Under ED conditions, the ion transport number represents the fraction of the current carried by that specific ion. The transport number of each ion can be derived from the concentration changes in compartments A and B. The (absolute) concentration change in compartment B (here an increase) is the same as the (absolute) concentration change in compartment A (here a decrease), if both compartments have equal volume. Therefore, during the experiments, samples of 1 mL were taken from both compartments at a certain time interval. The ion concentrations were determined by ion chromatography (IC, Metrohm Compact IC 761), at a confidence level of >95%.

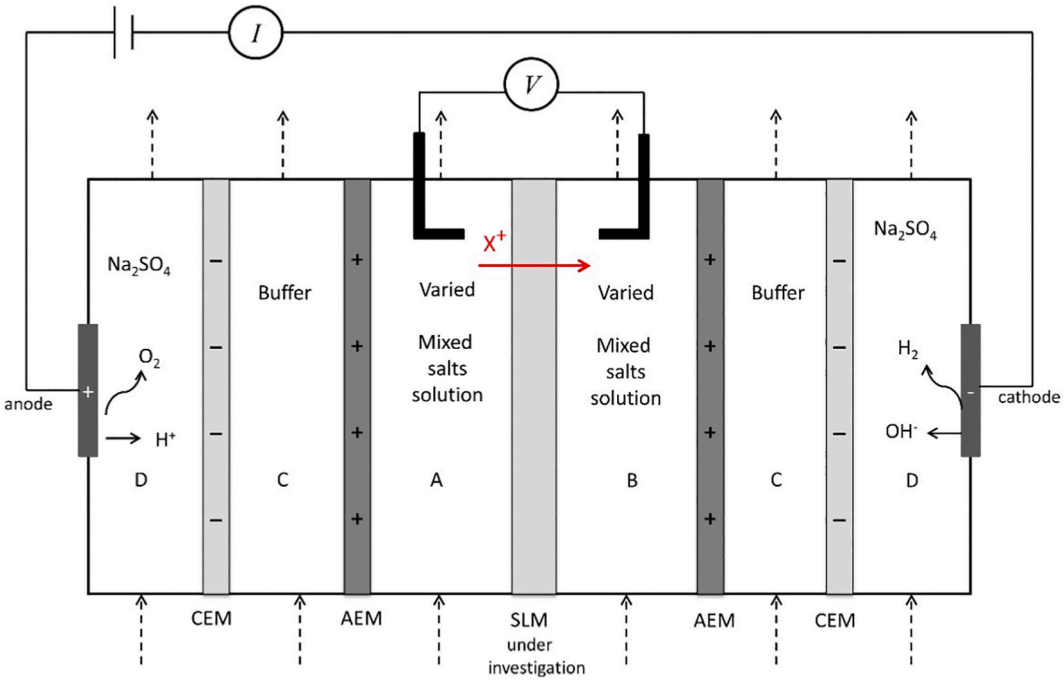

Fig. 1. Schematic of the configuration of the six-compartment cell used during the electro-dialysis (ED) experiments. Compartment C and D as well as the position of the CEMs and AEMs prevent the concentration changes in the two inner testing compartments from any interferences. As a result, the concentration changes of the cation species of interest in compartments A and B are solely due to transport of the central SLM.

The transport number t_i for ion species i is given by [37]:

$$t_i = \frac{zFV\frac{\Delta C}{\Delta t}}{I_{tot}A} \tag{1}$$

where z is the charge of the ion, F is the Faraday constant (96,485 C·mol^{-1}), V is the volume (m^3) of the feed or receiving compartment, A represents the effective membrane surface area (m^2), and I_{tot} is the (constant) externally applied current density (A·m^{-2}). The number of moles of the ion i transferred over the SLM per unit time, $\Delta C/\Delta t$ (mol·m^{-3}·s^{-1}), was calculated from the concentration change in compartment A. Note that here the decrease in concentration in compartment A is the same with the increase of concentration in compartment B.

For ions moving through the membrane, the molar ion flux is expressed as:

$$J = -u_i c_i \frac{dE_m}{dx} \tag{2}$$

where u_i (m^2·V^{-1}·s^{-1}) is the electrophoretic mobility of the ion i in the membrane, c_i represents the ion concentration in the membrane (in mol·m^{-3}). The SLM is overall electro-neutral. Based on the overall electroneutrality of the SLM, the borate concentration determines the concentration of exchanged cations. For the monovalent cations that is equal to the borate concentration (50 mM) and for the divalent cations that is half of the borate concentration (25 mM). Because of the relatively high dielectric constant of NPOE ($\varepsilon = 24$), intimate ion-pair formation between the borate and the cation is not considered [38,39]. By implication, the free, mobile cation concentration in the SLM equals the total cation concentration. dE_m/dx (V·m^{-1}) is defined as the electric field gradient.

Based on the electro-migration term in the Nernst-Planck equation, the current carried by ion species i is:

$$t_i I_{tot} = -zu_i c_i F \frac{dE_m}{dx} \tag{3}$$

I_{tot} represents the (total) current density. The effective membrane area is determined by the porosity Φ. In addition, the actual distance that the ion needs to travel through the SLM is larger than the membrane thickness, which is determined by the membrane tortuosity, τ. The electric field strength over the membrane should then be expressed as: $\frac{E_m}{\tau d}$, where E_m (V) is the recorded voltage drop over the membrane of thickness d (m). Therefore, Eq. (3) will be expressed as:

$$\frac{t_i I_{tot}}{\Phi} \times \tau = \varsigma t_i I_{tot} = zu_i c_i F \frac{E_m}{d} \tag{4}$$

where ς is a correction factor determined by the porosity and tortuosity of the ACCUREL membrane support, here determined to be $\varsigma = \frac{\tau}{\Phi} = \frac{2.1}{0.7} = 3$.

The electrophoretic ion mobility u_i of ion species i in the membrane determined from single-salt ED experiments, can then be given by:

$$u_i = \varsigma \frac{t_i I_{tot}}{zc_i F \frac{E_m}{d}} \tag{5}$$

The concentration of counter ions in the membrane (c) equals the borate concentration (A$^-$) divided by the valence of the counter ion. After substituting $c = \frac{A^-}{z}$ in Eq. (4), the mobility ratio $\frac{u_1}{u_2}$ of two ion species as assessed in single-salt solutions scales with t_1/t_2 and $E_{m,2}/E_{m,1}$ and is independent of their charge z.

2.4. Karl Fischer titration

Karl Fisher titration (Metrohm 756 KF Coulometer) was employed for determining the water concentration present in the pure organic solvent phase (NPOE) and in the presence of the lipophilic borate anion and equilibration with the different investigated salt solutions at room temperature. First fixed volumes of pure NPOE and NPOE containing the lipophilic anion A as the sodium salt were equilibrated the same fixed volumes (0.5 mL) of aqueous salt solutions containing 100 mM of NaCl, KCl, $CaCl_2$ and $MgCl_2$. Equilibration with Milli-Q water was used as reference. After equilibration, a sample size of 50 μg of the organic solvent was taken for the determination of the water content. The

amount of water (g) in the sample can be calculated based on the wt% results from the measurements. All experiments were performed in triplicate and standard deviation (STD) of the measured samples were calculated to determine the accuracy of the measurements. Ion concentrations of the salt solutions were determined by IC for monitoring the extent of ion exchange.

3. Results & discussion

3.1. Mass and charge balance

Ideally, when using the six-compartment cell shown in Fig. 1, the concentration changes of the, in this case, cation species in the two inner compartments A and B can solely be ascribed to ion transport over the membrane under investigation. Therefore, the change in compartment B is of the same magnitude as the change in compartment A but of opposite sign. In addition, in order to retain electro-neutrality, the total charge in each compartment should add up to zero. The mass and charge balance for all measurements in this study, including using (1): single-salt solutions of 100 mM KCl, NaCl, $CaCl_2$ and $MgCl_2$, (2): binary salt solutions of equimolar (50 mM) KCl + $CaCl_2$, KCl + $MgCl_2$ or $CaCl_2$ + $MgCl_2$, and (3): four ion mixed-solution of equimolar (25 mM) KCl + NaCl + $CaCl_2$ + $MgCl_2$ were determined and detailed data can be found in the Supplementary Information. Indeed, in all three sets of ED tests, the mass and charge balance were essentially closed.

3.2. Ion exchange at the water-membrane interface

Consider the presence of ion species M_1 of valence z_1 in the water or feed phase (f) and ion species M_2 of valence z_2 in the membrane phase (m). The ion-exchange process at the water-membrane interface can be expressed by:

$$z_2 M_{1,f} + z_1 M_{2,m} \overset{K_{ex}}{\rightleftarrows} z_2 M_{1,m} + z_1 M_{2,f} \quad (6)$$

K_{ex} represents the ion exchange constant, given by:

$$K_{ex} = \frac{M_{1,m}^{z_2} \times M_{2,f}^{z_1}}{M_{1,f}^{z_2} \times M_{2,m}^{z_1}} \quad (7)$$

Due to electroneutrality, the maximum total ion concentration in the membrane is determined by the impregnated lipophilic anion borate (A^-) concentration (50 mM). Therefore, the sum of positive charges from cations in the membrane equals the sum of negatively charges from the borate A^-:

$$z_1 M_{1,m} + z_2 M_{2,m} + z_A A = 0 \quad (8)$$

with z_A the charge of the membrane-bound anion (−1).

The cation partitioning in the membrane relates to the Gibbs free energy required for the translocation of an ion species of charge z and crystal radius r (in Å) from phase 1 with permittivity ε_1 to phase 2 with permittivity ε_2, as given by the Born equation [40,41]:

$$\Delta G = \frac{N_A z^2 e^2}{8\pi\varepsilon_0 r}\left(\frac{1}{\varepsilon_2} - \frac{1}{\varepsilon_1}\right) \quad (9)$$

with ΔG in kJ·Mol^{-1}, N_A Avogadro's number (6.02×10^{23}), e the elementary charge (1.6022×10^{-19}C) and ε_0 the permittivity of vacuum (8.854×10^{-12} F·m^{-1}). For transferring a monovalent cation ($z = 1$) from the aqueous phase ($\varepsilon_1 = 80$) into the NPOE/membrane phase ($\varepsilon_2 = 24$) [38,39]. Eq. (9) can be simplified into $\Delta G = 20.3/r$. And for divalent cations ($z = 2$), this will be $\Delta G = 81.2/r$.

Table 1 lists the crystal radii and the calculated ΔG values for complete ion dehydration according to the Born equation of the two monovalent cations Na^+ and K^+ and for the two divalent cations Ca^{2+} and Mg^{2+} used in this study.

The partitioning of two ion species M_1 and M_2 over the water phase and the organic solvent membrane phase is defined by a Boltzmann distribution. Assuming complete dehydration, the ion concentration ratio M_2 in the membrane, $M_{1,m}/M_{2,m}$ is defined as:

$$\frac{M_{1,m}}{M_{2,m}} = \frac{M_{1,f}}{M_{2,f}} exp\left(\frac{\Delta G_{M_2} - \Delta G_{M_1}}{RT}\right) \quad (10)$$

with the ΔG values calculated according to the Born equation.

Table 1
Crystal radii (in Å) of Na^+, K^+, Ca^{2+} and Mg^{2+}, as well as the calculated Born ΔG (in kJ mol^{-1}) required for the transfer of the particular ionic species from the aqueous into the NPOE/membrane phase.

	Crystal radius (in Å) [42,43]	ΔG (in kJ mol^{-1})
Na^+	0.95	21.4
K^+	1.33	15.3
Mg^{2+}	0.65	124.9
Ca^{2+}	0.99	82.0

3.3. Ion mobility in single-salt solutions

Flux measurements in symmetrical 100 mM NaCl, KCl, $CaCl_2$ or $MgCl_2$ solutions were used to determine the electrophoretic mobility of each ion species in the SLM. Fig. 2 shows the normalized Na^+, K^+, Ca^{2+} and Mg^{2+} concentration (the ratio of measured cation concentration and the initial cation concentration in the feed compartment A) over time and the linear fittings for all four ion species.

For all four tested cation solutions, the normalized cation concentration exhibits a linear decrease over time that is similar for cations of the same valence, whereas the slope for monovalent cations Na^+ and K^+ are determined as −0.00664 and −0.00678, respectively and for divalent cations Ca^{2+} and Mg^{2+} are −0.00362 and −0.00363, respectively. Because of the charge difference of two and the same current density applied, the decrease in normalized concentration of divalent cations is half of that found for the monovalent cations, which is also reflected by the ratio of the slopes of the plots.

The transport number of each ion (Eq. (1)) can be derived from the data shown in Fig. 2. The transport number and recorded voltage drop over the SLM (E_m/d) allow the calculation of ion mobility in the membrane (u), according to Eq. (5). The calculated ion mobility strongly

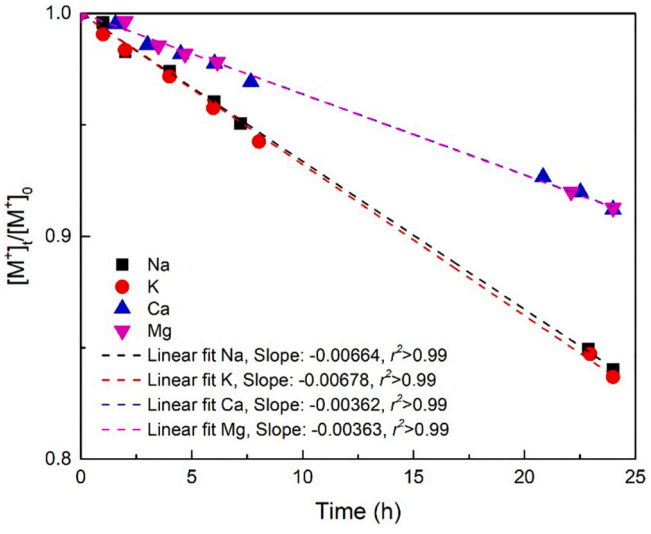

Fig. 2. Normalized Na^+, K^+, Ca^{2+} and Mg^{2+} concentrations in the feed compartment A, recorded over time in symmetrical 100 mM NaCl, KCl, $CaCl_2$ or $MgCl_2$ solutions. Also indicated the linear fits of the data, including the slope and regression coefficient r^2.

depends on the accuracy of the recorded membrane potential, hence the reported standard deviation (SD) values. Table 2 summarizes the calculated ion transport number (t_{ion}), recorded membrane potential drop (E_m/d) and calculated ion mobility (u_i).

As expected, and given that all transport numbers are close to unity (see Section 2.3.2), the mobility ratio of any couple of ions, u_1/u_2, (more or less) scales with the inverse of the corresponding measured membrane potentials, $E_{m,2}/E_{m,1}$. The electrophoretic mobility can also be expressed by [44]:

$$u_i = \frac{ez_i}{6\pi\eta r_i} \quad (11)$$

where e is the elementary charge, η (Pa·s) is the viscosity of the solvent and r_i (m) is the radius of the ion. As shown in Eq. (11), the electrophoretic mobility of an ion relates to its size, whether it is dehydrated or hydrated. If dehydrated, the mobility is expected to scale with the reciprocal ion crystal radius, if hydrated, with the reciprocal hydrated radius. According to Eq. (11), z/u is linear with r, with a slope of e/6πη (in $m^3 \cdot V^{-1} \cdot s^{-1}$). As reported before [20], the mobility ratio of K^+ and Na^+ is rather close to the reciprocal ratio of their crystal radii, reflecting that these monovalent cations are present in the SLM essentially completely dehydrated. Fig. 3 shows the correlation of the ion crystal radius of K^+ and Na^+ with their charge and mobility (z/u) ratio (solid line), with the electrophoretic mobility values taken from Table 3. Based on theoretical considerations, the (extended) linear fit through the Na^+ and K^+ data points was forced to go through the origin. As remarked, Eq. (11) should hold irrespective the hydration state of the particular ion species. Therefore, the plot in Fig. 3 has been extrapolated to z/u values of Ca^{2+} and Mg^{2+} (dotted line), again using the u values from Table 3. The in this way obtained radius of Ca^{2+} ($r_{p,Ca}$) and Mg^{2+} ($r_{p,Mg}$) is 2.68 Å and 3.96 Å, respectively, values clearly larger than the crystal radii listed in Table 1. However, the slope derived from Fig. 3 is 3×10^{-20} $m^3 \cdot V^{-1} \cdot s^{-1}$, resulting in a viscosity η of the NPOE-borate system of 0.28 Pa·s, a value about 20 times higher than the reported value of 0.0137 Pa·s for pure NPOE [45]. Possible explanations for this observed difference include: (1) The actual concentration of free cations in the SLM. It is important to realize that all mobility calculations assume the cations to be present in the SLM as free, mobile charge carriers. For instance, given a borate concentration of 50 mM, the free cation concentration in the SLM was assumed to be 50 mM and 25 mM in pure NaCl or $CaCl_2$ solutions, respectively. We cannot rule out however that the borate interacts with the cations. The effect would be that at any moment in time only a fraction of the cations present contribute to the (constant) total applied current with the remaining fraction essentially temporarily immobilized. The extent of interaction may be cation species dependent. Even though this effect is expected to be more dominant for the divalent cations, their hydration shell, enlarging their effective radius, counteracts the higher charge regarding the electrostatic interaction with borate. One way to reconcile the high viscosity derived from Fig. 3 and the much lower viscosity of pure NPOE is to assume that only 5% of the cations are free to move, implying an actual mobility 20 times higher than the ones calculated and listed in Table 2. This, in turn, results in a slope ($=r \times u/z$) of Fig. 3 also 20 times higher and with that a 20 times lower viscosity (slope = 6πη/e). (2) The actual viscosity of NPOE/borate is affected by an interaction with the membrane (Accurel) pore wall.

Table 2
Transport numbers of Na^+, K^+, Mg^{2+} and Ca^{2+} (t_{ion}), recorded membrane potential drop (E_m/d) with SD, and the ion mobility in the membrane (u_i) with SD, all derived from single salt ED measurements.

	t_{ion}	$E_m/d \times 10^{-4}$ ($V \cdot m^{-1}$)	SD $E_m/d \times 10^{-4}$ ($V \cdot m^{-1}$)	$u_i \times 10^{10}$ ($m^2 \cdot V^{-1} \cdot s^{-1}$)	SD $u_i \times 10^{10}$ ($m^2 \cdot V^{-1} \cdot s^{-1}$)
Na^+	0.97	1.6	0.04	3.60	0.09
K^+	0.93	2.8	0.12	2.17	0.09
Mg^{2+}	0.98	2.7	0.06	2.26	0.05
Ca^{2+}	0.98	4.0	0.17	1.52	0.06

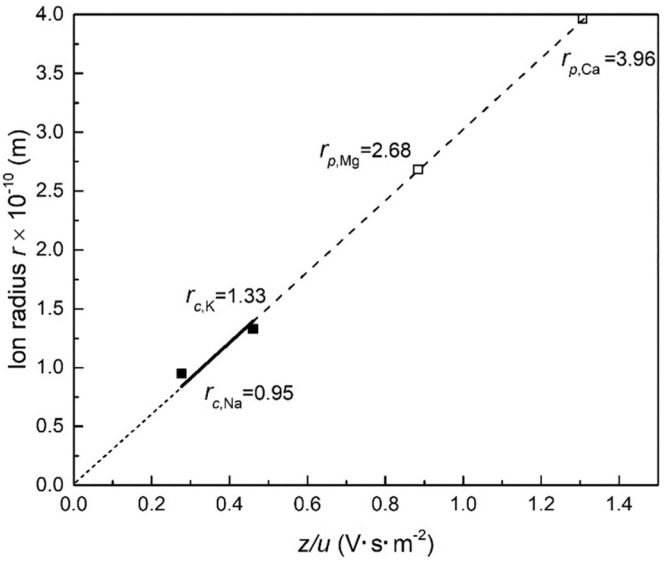

Fig. 3. Correlation between the ion radius r and the ratio of charge and mobility (z/u) for K^+, Na^+, Ca^{2+} and Mg^{2+}. $r_{c,Na}$ and $r_{c,K}$ represent the crystal radius of Na^+ and K^+, $r_{p,Ca}$ and $r_{p,Mg}$ the predicted (partially hydrated) radius of Ca^{2+} and Mg^{2+}. The (extended) linear fit through the Na^+ and K^+ data points was forced to go through the origin because of theoretical considerations.

Table 3
Measured mean water content (wt%) in pure NPOE after equilibration in pure water and in 100 mM NaCl, KCl, $MgCl_2$ and $CaCl_2$ solutions. Average values and standard deviations (SD) are based on measurements in triplicate.

Pure NPOE equilibrated with	C_{salt} (mM)	Measured water (wt%)	SD	C_{water} (mM)
H_2O	0	0.12	0.01%	69
NaCl	100	0.12	0.00%	69
KCl	100	0.11	0.02%	64
$MgCl_2$	100	0.11	0.00%	69
$CaCl_2$	100	0.12	0.02%	64

The data of Fig. 3 indicate that, in contrast to monovalent cations, divalent cations are still partly hydrated while traversing the SLM. For that reason, next the amount of water taken up by the SLM was investigated, with the water present as hydration water of the divalent cations.

3.4. Water content in NPOE

Quantification of the water content in the organic solvents (NPOE or NPOE with lipophilic anion A) after equilibration with water or with different salt solutions was performed by using the standard coulometric Karl Fischer (KF) titration method. Measurements were performed in triplicate. As the lipophilic anion A^- was impregnated in NPOE as a sodium salt, the same (calculated) amount of the Na^+ in the organic solvent was found in the aqueous solution after equilibration, indicating a full ion exchange of the cation species in the membrane. Tables 3 and 4 list the measured water content (wt%) in pure NPOE or NPOE containing lipophilic anion A^-, respectively, and the calculated amount of water C_{water} (in mM) for each sample. The SD values for all samples ≤0.02% indicates the rather high reproducibility of the KF measurements. Clearly, from Table 3, compared to the water content of the sample equilibrated in pure water, adding either 100 mM NaCl, KCl, $CaCl_2$ or $MgCl_2$ to the equilibration solution has no effect. The calculated amount of water in all samples is about the same (64–69 mM, based on 0.11–0.12 wt%).

Table 4
Measured mean water content (wt%) in the NPOE in the presence of the lipophilic anion A^- (50 mM borate) after equilibration in pure water or 100 mM NaCl, KCl, $MgCl_2$ and $CaCl_2$ solutions. Average values and standard deviations (STD) are based on measurements in triplicate.

NPOE + A^- equilibrated with	C_{salt} (mM)	Measured water (wt%)	SD	C_{water} (mM)
H_2O	0	0.35	0.01%	137
NaCl	100	0.34	0.01%	127
KCl	100	0.33	0.02%	127
$MgCl_2$	100	0.53	0.00%	243
$CaCl_2$	100	0.50	0.02%	220

As shown in Table 4, in pure water, adding A^- (present as Na^+ salt) to the NPOE doubles the water concentration in the SLM, from 69 to 137 mM. Adding either NaCl or KCl to the feed solution has no effect on the final water content of the NPOE. Apparently, either hydrated Na^+ from the feed is exchanged for hydrated Na^+ leaving the SLM or, alternatively, the exchange involves the two ions dehydrated. In both cases, the water content of the SLM remains the same. Based on this data alone we cannot distinct between these two scenarios. However, the mobility – ion radius relation make us conclude that monovalent cations traverse the SLM in the dehydrated state. In contrast, with $MgCl_2$ or $CaCl_2$ present in the feed, the final water concentration almost doubles. Compared to the control of Table 3 and with A^- included in the SLM, the presence of $CaCl_2$ or $MgCl_2$ in the feed solution increased the water concentration of approximately 160 mM. Considering a Ca^{2+}/Mg^{2+} concentration of 25 mM (given the A^- of 50 mM), the (average) hydration number of each divalent cation-borate complex would be around 6.5. The increased water content due to the exchange of Mg^{2+} with Na^+ initially associated with the borates is 243–127 = 116 mM per 50 mM borate sites, and is slightly higher than Ca^{2+} of 220–127 = 93 mM per 50 mM borate site. This is also in line with stronger hydration by the smaller crystal radius of Mg^{2+}. Because the water involved in the hydration of A^- is ignored, this value is slightly overestimated. Considering the reported range of hydration numbers of Ca^{2+} and Mg^{2+} of 5–12 [37–40], this indicates that these divalent cations indeed have lost part of their water shell, consistent with the conclusion based on the relation mobility ratio and ion radius (Fig. 3).

A final remark on the water content of NPOE concerns the presumed linearity between z/u and r, Eq. (11), a relationship constrained by a constant viscosity of the SLM. It is very well conceivable that the uptake of water alters the overall viscosity of the SLM system. However, given an NPOE concentration of approximately 4 M and water concentration differences in the order of 0.1 M, the assumption of constant viscosity seems justified.

3.5. Ion exchange

3.5.1. Determination of the ion-exchange selectivity constant in binary salt solutions

Ion permeation through an ion-exchange membrane by ED relates to both ion exchange of the particular ionic species over the biphasic water – membrane system and ion electrophoretic mobility through the membrane. The previous paragraphs addressed the extent of hydration

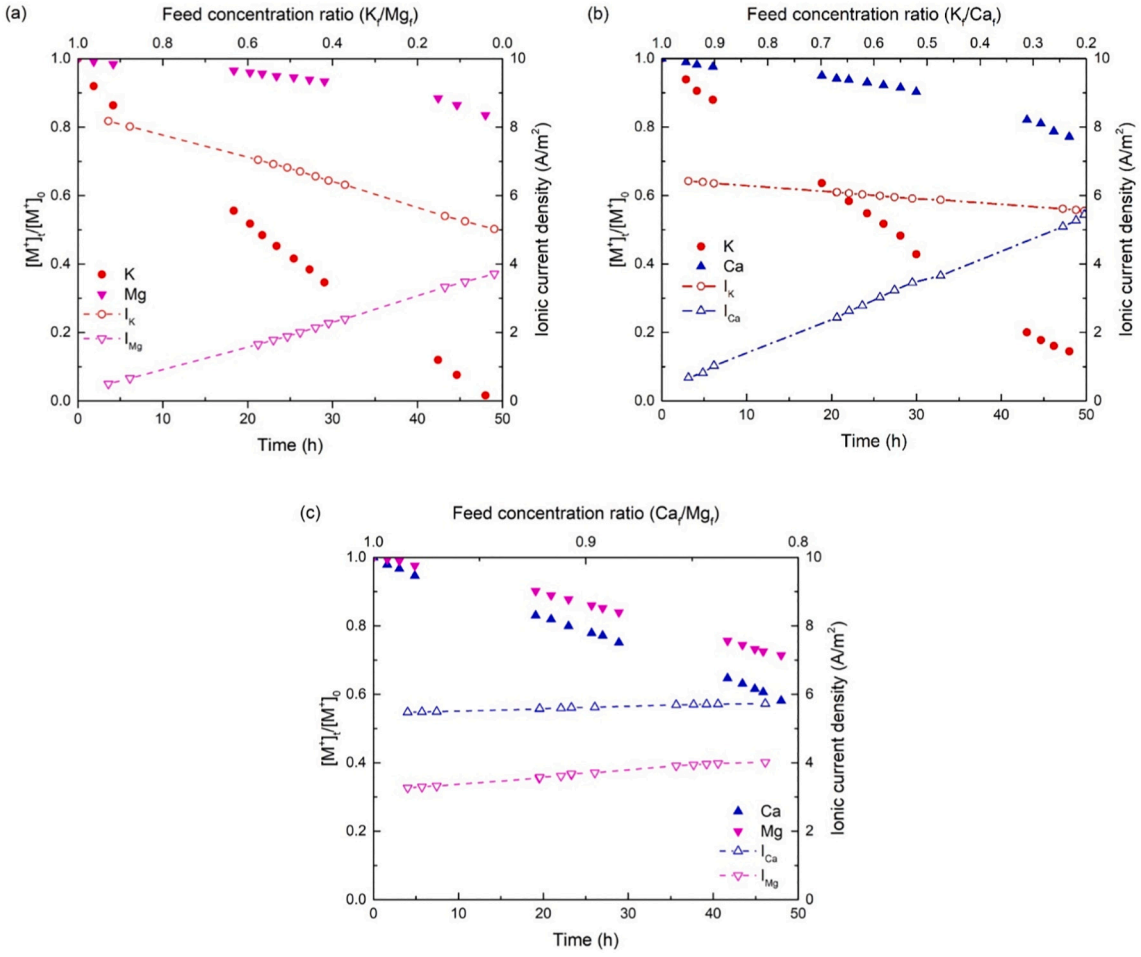

Fig. 4. Normalized feed concentration ratios (left axis) and ionic currents (right axis) *versus* time as measured in symmetrical binary salt solutions of (a) 50 mM KCl + 50 mM $CaCl_2$, (b) 50 mM KCl + 50 mM $MgCl_2$ and (c) 50 mM $CaCl_2$ + 50 mM $MgCl_2$.

on the electrophoretic ion mobility in single-salt experiments. This paragraph focusses on the electro dialysis of binary and multi-ion solutions to determine and understand the ion-exchange process.

As the total charge of the permeating cations in the membrane is equal to the charge carried by the present lipophilic anions, different cations will actually compete with each other to enter or to leave the SLM in the case of mixed-salt solutions in the feed phase.

Fig. 4 shows how the ion concentrations in the feed compartment A change in time during 48 h starting with binary equimolar mixtures (50 mM each) of KCl and $MgCl_2$ (Fig. 4a), KCl and $CaCl_2$ (Fig. 4b), and $CaCl_2$ and $MgCl_2$ (Fig. 4c). The changing ion concentrations are presented as normalized ion concentrations (left-hand axis). From the ion concentrations in the feed, the ionic current densities were calculated, which are also presented in Fig. 4 (right-hand axis). The sum of the calculated transport numbers of the two cations involved in each series is 0.88 (Fig. 4a), 1 (Fig. 4b), and 0.98 (Fig. 4c). These numbers indicate that under these conditions the current through the SLM is predominantly carried by the cations. For the binary mixture of KCl and $MgCl_2$, lower transport number of 0.88 was found, indicating that part of the current is carried in another way. The transport of protons was excluded because we did not detect a pH change in the feed and receiving phase compartments. It is speculated that, despite the cation-exchange properties of the SLM, some chloride might be counter transported. We have not investigated further this possibility.

Clearly, as seen from Fig. 4a and b, K^+ is transported right from the start with the K^+ current gradually decreasing over time. In contrast, both the Mg^{2+} and Ca^{2+} transport is close to zero at the start and increased over time.

For a K^+/Mg^{2+} feed ratio of 0.2 (as observed after about 38 h; thus about 10 h earlier compared to the K^+/Ca^{2+} situation; see below), the current ratio is 5.8: 3, reflecting a molar permeation ratio of 1:0.26. While for the mixture of K^+/Ca^{2+}, after 48 h, the K^+ current equals the Ca^{2+} current, indicating that at K^+/Ca^{2+} feed concentration ratio of about 0.2, the K^+/Ca^{2+} permeation ratio is about 1:0.5. By comparing these data, it is clear that Mg^{2+} is much less competitive compared to Ca^{2+} in the electro-dialysis with K^+. Also, in the combined Ca^{2+}/Mg^{2+} experiment (Fig. 4c), we have observed a preference of Ca^{2+} permeation compared to Mg^{2+} permeation. This difference cannot be explained by the different mobilities of Mg^{2+} and Ca^{2+}, since we have observed (Table 2) that Mg^{2+} is more mobile compared to Ca^{2+}. Therefore, the difference originates from the difference in ion-exchange selectivity $K_{ex}(K^+/Mg^{2+})$ and $K_{ex}(K^+/Ca^{2+})$.

We will focus now on the extraction of the ion-exchange selectivity constants from our electro-dialysis data.

According to Eq. (4), the ratio of current carried by ion species M_1 and M_2 equals:

$$\frac{I_{M_1}}{I_{M_2}} = \frac{z_1 M_{1,m} u_{M_1}}{z_2 M_{2,m} u_{M_2}} \tag{12}$$

with $M_{1,m}$ and $M_{2,m}$ the concentrations of M_1 and M_2 in the membrane ($mol \cdot m^{-3}$).

For experiments involving two monovalent or the two divalent cations, (*i.e.* $z_1 = z_2$), Eq. (12) equals:

$$\frac{M_{1,m}}{M_{2,m}} = \frac{I_{M_1}}{I_{M_2}} \times \frac{u_{M_2}}{u_{M_1}} \tag{13}$$

The general derived equation for the ion-exchange selectivity constant K_{ex} as given in Eq. (7) simplifies for two monovalent cations and for two divalent cations to:

$$K_{ex} = \frac{M_{1,m} \times M_{2,f}}{M_{1,f} \times M_{2,m}} = \frac{M_{1,m}}{M_{2,m}} \times \frac{M_{2,f}}{M_{1,f}} \tag{14}$$

Substituting Eq. (13) into Eq. (14) gives:

$$K_{ex} = \frac{I_{M_1}}{I_{M_2}} \times \frac{u_{M_2}}{u_{M_1}} \times \frac{M_{2,f}}{M_{1,f}} \tag{15}$$

In this case K_{ex} is dimensionless. The factor $\frac{I_{M_1}}{I_{M_2}} \times \frac{u_{M_2}}{u_{M_1}}$ is equal to $\frac{M_{1,m}}{M_{2,m}}$.

For a binary mixture containing one monovalent cation ($M_1 = K^+$; $z_1 = 1$) and one divalent cation ($M_2 = Ca^{2+}$ or Mg^{2+}; $z_2 = 2$), the situation is more complex. $\frac{M_{1,m}^{z_2}}{M_{2,m}^{z_1}}$ in Eq. (7) is expressed by:

$$\frac{M_{1,m}^2}{M_{2,m}} = \frac{I_{M_1}^2}{I_{M_2}} \times \frac{u_{M_2}}{u_{M_1}^2} \times \frac{2d}{FE_m} \tag{16}$$

Resulting in an expression of K_{ex} as a function of:

$$K_{ex} = \frac{M_{1,m}^2}{M_{2,m}} \times \frac{M_{2,f}}{M_{1,f}^2} = \frac{I_{M_1}^2}{I_{M_2}} \times \frac{u_{M_2}}{u_{M_1}^2} \times \frac{2d}{FE_m} \times \frac{M_{2,f}}{M_{1,f}^2} \tag{17}$$

According to Eq. (7), plotting $M_{1,m}^{z2}/M_{2,m}^{z1}$ as function of $M_{1,f}^{z2}/M_{2,f}^{z1}$ renders a graph with slope K_{ex}.

We have plotted our experimental data for the binary combinations K^+/Na^+ (earlier published by us [20]) and Ca^{2+}/Mg^{2+} according to Eq. (15). The results are shown in Fig. 5a and b. For both combinations we observed, as expected, a linear fit. Based on theoretical considerations, the fit was forced to go through the origin. From the slopes of the plots we deduced the values for the ion-exchange selectivity constants $K_{ex}(K^+/Na^+) = 12.7$ and $K_{ex}(Ca^{2+}/Mg^{2+}) = 2.6$. As becomes clear by comparing Eqs. (10) and (14), the exponential term in Eq. (10) represents K_{ex}, thus providing, apart from Eq. (14)/Eq. (15), a second expression for K_{ex}, at least in the case of two monovalent cation species that require total dehydration. Indeed, the K_{ex} value of 11.7 calculated from Eq. (10) [20] nicely corresponds to the value of 12.7 after applying Eq. (15).

Next, we plotted our experimental data for the binary combinations K^+/Mg^{2+} and K^+/Ca^{2+} according to Eq. (17) (Fig. 6). We do indeed observe in both cases a linear plot (forced passing the origin) for $M_{1,f}^{z2}/M_{2,f}^{z1} < 25$. However, for the initial part of these experiments (where the feed ratios of K^+ to Mg^{2+} or to $Ca^{2+} > 0.6$), *i.e.* the upper right part in Fig. 6a and b our data points deviate from the linear part. The use of K_{ex} values assumes chemical equilibrium. Therefore, this observed deviation may reflect that equilibrium has not (yet) established. For one thing, at the start of the experiment the concentration of divalent cations in the SLM will be virtually zero, implying that the exchange of *e.g.* Ca^{2+} from the feed and Na^+ in the SLM occurs in one direction. In addition, it is well-known that membrane selectivity is not a fixed parameter but instead varies with changing ionic conditions in the feed and/or receiving solution, as is the case in a dynamic system as ours. From the linear part we first derived the ion-exchange selectivity constants of $K_{ex}(K^+/Mg^{2+}) = 10.6$ and $K_{ex}(K^+/Ca^{2+}) = 2.9$ from the slopes. From these two K_{ex} values, we can easily calculate and (expected) value of $K_{ex}(Ca^{2+}/Mg^{2+}) = 3.6$. This is very close to the obtained value of $K_{ex}(Ca^{2+}/Mg^{2+}) = 2.6$ from the experiment using the binary Ca^{2+}/Mg^{2+} mixture. This gives us confidence in the linear relation of the latter stage of the experiment. The data points strongly deviating from the linear plots $M_{1,f}^{z2}/M_{2,f}^{z1} > 35$ are both related to the start of the experiments using feed mixtures containing K^+ and Mg^{2+} or Ca^{2+}. For some reasons in the initial stage of these experiments, the permeation through the membrane is much more favorable for K^+ compared to the later stage of the experiment. For now, we can only speculate about the reason causing this deviation. The calculation of K_{ex} is based on the assumption of chemical equilibrium. Apparently, during the first 5 h or so of the experiment the equilibrium state is not reached yet. In addition, it might be that for some reason in ion mixtures involving both monovalent and divalent cations, K_{ex} is more sensitive to the K^+ concentration in the feed.

In Table 5 the obtained ion-exchange selectivity constants are tabulated.

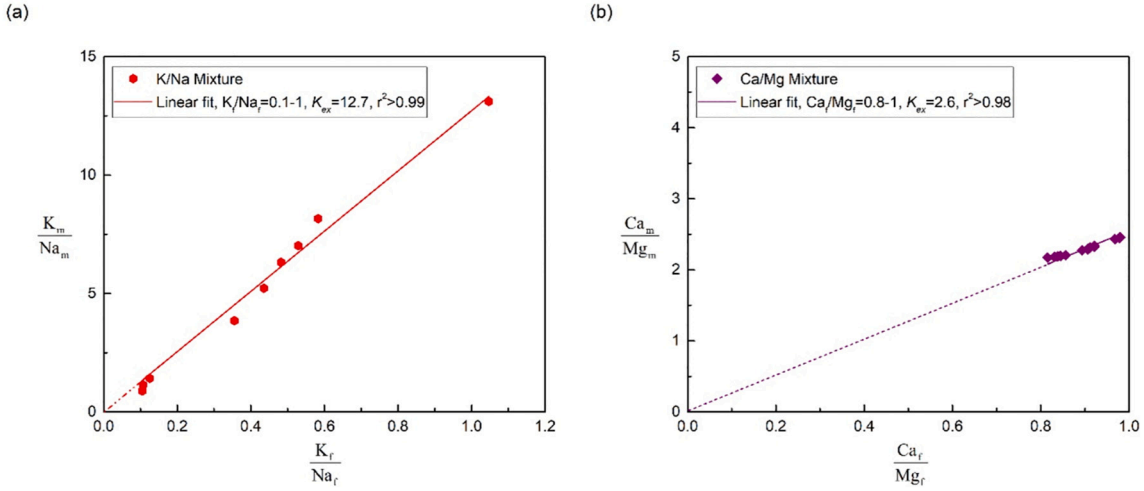

Fig. 5. The ion-exchange selectivity constant of two ion species in binary ion solutions ($M_1 = K^+$ or Ca^{2+} $M_2 = Na^+$ or Mg^{2+}) determined as the slope by plotting $\frac{M_{1,m}}{M_{2,m}}$ *versus* $\frac{M_{1,f}}{M_{2,f}}$ and the regression coefficient r^2. Fits were forced to go through the origin.

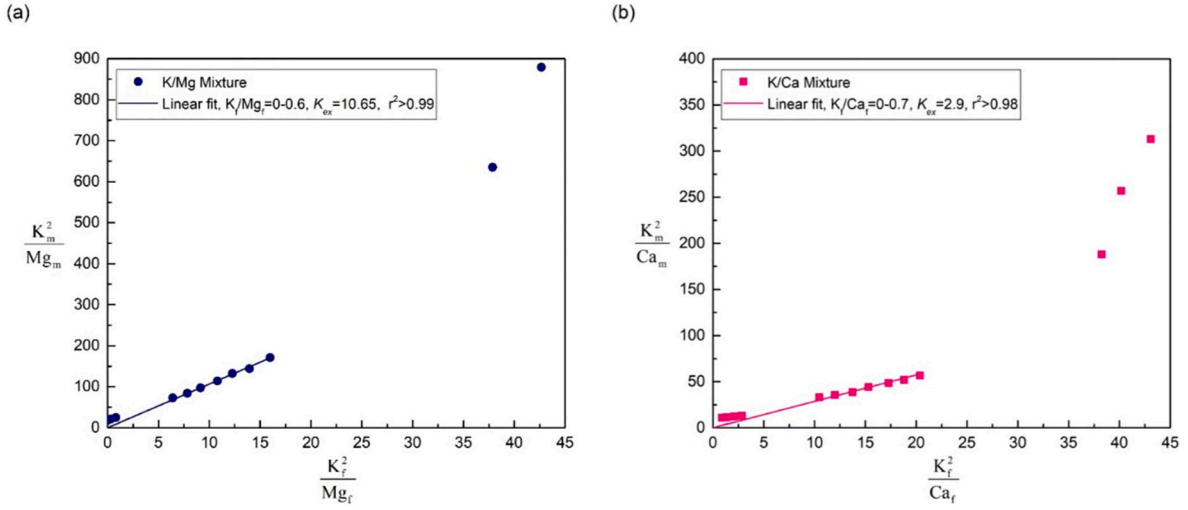

Fig. 6. The ion-exchange selectivity constant of two ion species in binary ion solutions ($M_1 = K^+$ or $M_2 = Mg^{2+}$ or Ca^{2+}) determined as the slope by plotting $\frac{M_{1,m}^2}{M_{2,m}}$ *versus* $\frac{M_{1,f}^2}{M_{2,f}}$ and the regression coefficient r^2. Fits were forced to go through the origin.

Table 5
Determined ion-exchange selectivity constant for the ion combination of K^+/Na^+, Ca^{2+}/Mg^{2+}, K^+/Ca^{2+} and K^+/Mg^{2+} in binary ion mixture or the quaternary ion mixture.

Ion exchange constant (K_{ex})	Binary mixture (Section 3.5.1)	Quaternary mixture (Section 3.5.2)
K^+/Na^+	12.6	11.3
Ca^{2+}/Mg^{2+}	2.6	3.3
K^+/Ca^{2+}	2.9	3.6
K^+/Mg^{2+}	10.6	12.8

3.5.2. Determination of the ion-exchange selectivity constant in quaternary solutions

Finally, we have investigated the electro-dialysis of an equimolar mixture (each at 25 mM) of NaCl, KCl, $CaCl_2$ and $MgCl_2$, to see if there is any cross-coupling effect between these different ions. This experiment was set up similarly as the experiments on the binary mixtures, discussed before.

Fig. 7 shows how the ion concentrations in the feed compartment A change in time during 48 h starting with the quaternary equimolar mixture (25 mM each) of NaCl, KCl, MgCl2 and $CaCl_2$. The changing ion concentrations are presented as normalized ion concentrations (left-hand axis). From the changing ion concentrations in the feed, the ionic current densities were calculated and are also presented in Fig. 7 (right-hand axis). The sum of the calculated transport numbers of the four cations involved is close to unity, and leads to the conclusion (as before) that under these conditions the current is predominantly carried by the cations.

It is observed that the dominant cation transported is K^+ and is followed by Na^+, Ca^{2+} and finally Mg^{2+}. This confirms the order observed before in the binary salt experiments, where K^+ is dialyzed in preference over Na^+ and where Ca^{2+} is dialyzed in preference over Mg^{2+}.

Similar to the analysis performed for the binary solutions, the K_{ex} values of the different ion combinations in the quaternary ion solution were determined and the results are shown in Fig. 8. Comparing the combination of K^+/Na^+ and Ca^{2+}/Mg^{2+}, from Fig. 8, we observed here a linear relation through the origin over the given entire concentration ratio range with the determined K_{ex} value of 11.3 and 3.3, respectively.

For the combination K^+/Ca^{2+} and K^+/Mg^{2+}, we also made similar observations as in the binary salt experiments. The plotted lines (forced through the origin) relate only to the later stage of the experiment.

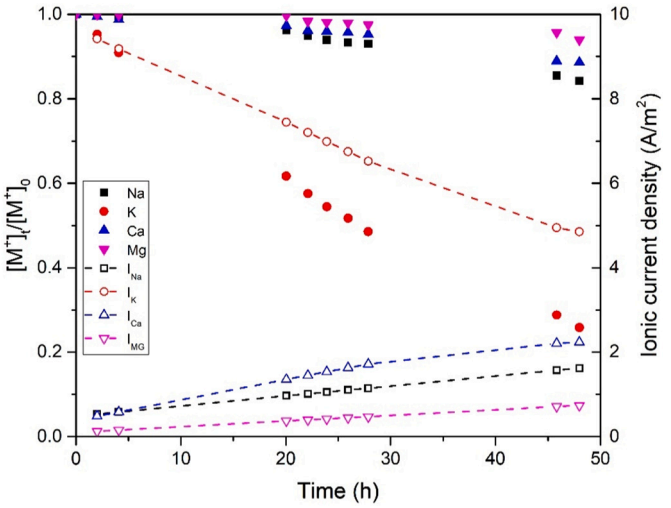

Fig. 7. Normalized Na^+, K^+, Ca^{2+} and Mg^{2+} concentrations and ionic current over time in symmetrical equimolar (25 mM) mixed-salt solutions.

Initially, also here a deviation from the linear plot was observed. The ion-exchange selectivity constants of $K_{ex}(K^+/Ca^{2+}) = 3.6$ and $K_{ex}(K^+/Mg^{2+}) = 12.8$ were obtained. All K_{ex} values obtained from the experiment using the quaternary salt mixture are also tabulated in Table 5 for comparison with the values obtained from the binary salt experiments. From this comparison it is remarkable to see the very good similarity of the obtained ion-exchange selectivity constant K_{ex} from both the binary and quaternary salt mixture experiments. This similarity shows that there is no interference between the different salts in that they pass the membrane independently. The ion-exchange selectivity constant (K_{ex} relative to K_{ex} of K^+) increases in the order: $Ca^{2+} < Mg^{2+} \approx Na^+$.

4. Conclusions

This study investigated in detail the permeation of K^+, Ca^{2+} and Mg^{2+} under electro-dialysis conditions with constant current applied using a supported liquid membrane (SLM). Single-salt experiments identified an electro-phoretic mobility decreasing in the order: $Na^+ > K^+ > Mg^{2+} > Ca^{2+}$. The relative order between the monovalent ions (Na^+ and K^+) and also between the divalent ions (Mg^{2+} and Ca^{2+}) correlate with their ionic radii. However, such a correlation does not exist if we compare the monovalent and the divalent cations. From our

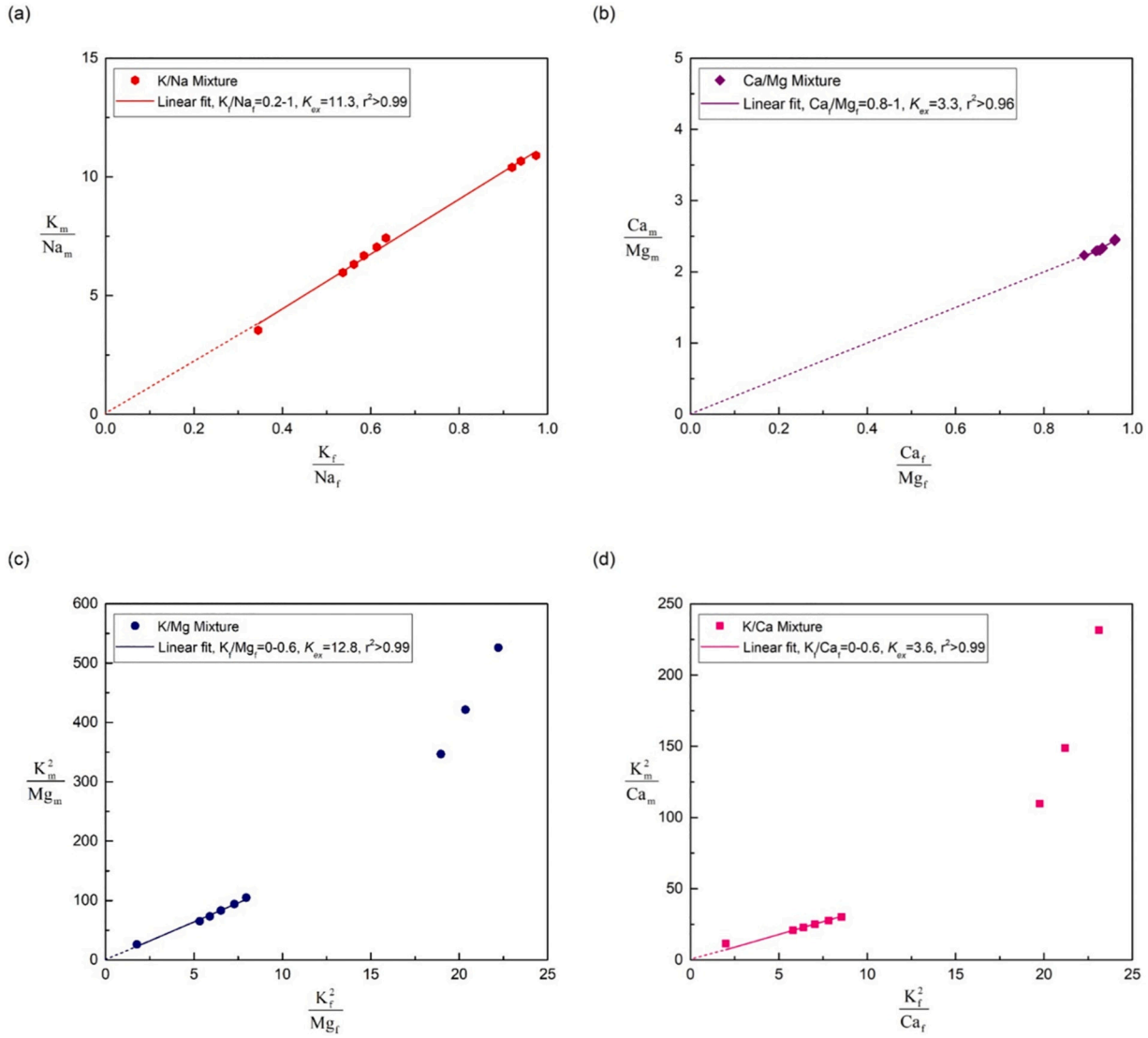

Fig. 8. The ion-exchange selectivity constant of two ion species in four ion mixed solution ($M_1 = K^+$, $M_2 = Na^+$, Mg^{2+} or Ca^{2+}) determined as the slope by plotting $\frac{M_{1,m}^{z_2}}{M_{2,m}^{z_1}}$ *versus* $\frac{M_{1,f}^{z_2}}{M_{2,f}^{z_1}}$ and the regression coefficient r^2. Fits were forced to go through the origin.

earlier study on the permeation selectivity between Na^+ and K^+ [20], we had found that these ions enter the SLM in a dehydrated state. Clearly, that is not the situation for the divalent cations investigated here. From a correlation between z/u *vs.* r, where z is the valence of the cation, u the observed electro-phoretic mobility and r the radius of the migrating cation known for Na^+ and K^+, and unknown for Mg^{2+} and Ca^{2+}, we obtained the predicted radii of the divalent cations. These higher radii were interpreted as due to the presence of a (partial) hydration shell around that cation. The main difference in the hydration state between the mono- and divalent cations in the SLM is related to the much higher dehydration energy of the divalent ions compared to the monovalent cations. The electrophoretic mobility of the divalent cations is thus determined by the radius of their (partly) hydrated state. Karl Fisher titrations confirmed the presence of additional water in the SLM after equilibration with divalent cations compared to monovalent cations.

From the binary and quaternary salt experiments we found a permeation selectivity in the order of: $K^+ > Na^+ > Ca^{2+} > Mg^{2+}$. Clearly, this order does not correlate with the observed electro-phoretic mobilities from the single-salt experiments. The origin of this difference can be found in cation exchange occurring at the water/SLM interface. The different cations compete for the lipophilic borate sites in the SLM, quantified by an ion-exchange selectivity constant K_{ex} value. Analysis revealed values of K_{ex} following the order of: $K^+ > Ca^{2+} > Mg^{2+} \approx Na^+$. Both K_{ex} and the electro-phoretic mobility in the SLM contribute to the observed permeation selectivity of the different cation species.

CRediT authorship contribution statement

Zexin Qian: Conceptualization, Investigation, Formal analysis, Data curation, Writing – original draft. **Henk Miedema**: Supervision, Conceptualization, Formal analysis, Data curation, Writing – review & editing. **Louis C.P.M. de Smet**: Supervision, Writing – review & editing. **Ernst J.R. Sudhölter**: Supervision, Conceptualization, Writing – review & editing.

Declaration of competing interest

The authors declare that they have no known competing financial interests or personal relationships that could have appeared to influence the work reported in this paper.

Acknowledgements

This work was performed in the cooperation framework of Wetsus, European Centre of Excellence for Sustainable Water Technology (www.wetsus.nl). Wetsus is co-funded by the Dutch Ministry of Economic Affairs and Ministry of Infrastructure and the Environment, the European Union Regional Development Fund, the Province of Fryslan and the Northern Netherlands Provinces. This work is part of a project that has received funding from the European Union's Horizon 2020 research and innovation program under the Marie Skfodowska-Curie grant agreement No 65874. The authors like to thank the participants of the research theme "Desalination" for the fruitful discussions and their financial support. A special word of thank goes to Van der Knaap (The Netherlands) and Yara (The Netherlands) for all their advice and support. L.C.P.M.d.S. acknowledges the European Research Council (ERC) for a Consolidator Grant, which is part of the European Union's Horizon 2020 research and innovation program (grant agreement No. 682444).

Appendix A. Supplementary data

Supplementary data to this article can be found online at https://doi.org/10.1016/j.desal.2021.115398.

References

[1] H. Strathmann, Electrodialysis, a mature technology with a multitude of new applications, Desalination 264 (2010) 268–288, https://doi.org/10.1016/j.desal.2010.04.069.
[2] A. Campione, L. Gurreri, M. Ciofalo, G. Micale, A. Tamburini, A. Cipollina, Electrodialysis for water desalination: a critical assessment of recent developments on process fundamentals, models and applications, Desalination 434 (2018) 121–160, https://doi.org/10.1016/j.desal.2017.12.044.
[3] S. Al-Amshawee, M.Y.B.M. Yunus, A.A.M. Azoddein, D.G. Hassell, I.H. Dakhil, H. A. Hasan, Electrodialysis desalination for water and wastewater: a review, Chem. Eng. J. 380 (2020), 122231, https://doi.org/10.1016/j.cej.2019.122231.
[4] T. Sata, T. Sata, W. Yang, Studies on cation-exchange membranes having permselectivity between cations in electrodialysis 206 (2002) 31–60, https://doi.org/10.1016/S0376-7388(01)00491-4.
[5] T. Luo, S. Abdu, M. Wessling, Selectivity of ion exchange membranes: a review 555 (2018) 429–454, https://doi.org/10.1016/j.memsci.2018.03.051.
[6] H. Zhang, P.K. Shen, Advances in the high performance polymer electrolyte membranes for fuel cells, Chem. Soc. Rev. 41 (2012) 2382–2394, https://doi.org/10.1039/c2cs15269j.
[7] M. Xie, H.K. Shon, S.R. Gray, M. Elimelech, Membrane-based processes for wastewater nutrient recovery: technology, challenges, and future direction, Water Res. 89 (2016) 210–221, https://doi.org/10.1016/j.watres.2015.11.045.
[8] J. Ran, L. Wu, Y. He, Z. Yang, Y. Wang, C. Jiang, L. Ge, E. Bakangura, T. Xu, Ion exchange membranes: new developments and applications 522 (2017) 267–291, https://doi.org/10.1016/j.memsci.2016.09.033.
[9] J.G. Hong, B. Zhang, S. Glabman, N. Uzal, X. Dou, H. Zhang, X. Wei, Y. Chen, Potential ion exchange membranes and system performance in reverse electrodialysis for power generation: a review 486 (2015) 71–88, https://doi.org/10.1016/j.memsci.2015.02.039.
[10] A. Parasuraman, T.M. Lim, C. Menictas, M. Skyllas-Kazacos, Review of material research and development for vanadium redox flow battery applications, Electrochim. Acta 101 (2013) 27–40, https://doi.org/10.1016/j.electacta.2012.09.067.
[11] L. Ge, B. Wu, D. Yu, A.N. Mondal, L. Hou, N.U. Afsar, Q. Li, T. Xu, J. Miao, T. Xu, Chin.J. Chem. Eng. 25 (2017) 1606–1615, https://doi.org/10.1016/j.cjche.2017.06.002.
[12] F. Gallucci, Encyclopedia of Membranes, Springer, 2016, https://doi.org/10.1007/978-3-662-44324-8.
[13] D.Ariono Khoiruddin, I.G.Wenten Subagjo, Surface modification of ion-exchange membranes: methods, characteristics, and performance, J. Appl. Polym. Sci. 134 (2017) 45540, https://doi.org/10.1002/app.45540.
[14] C. Cheng, N. White, H. Shi, M. Robson, M.L. Bruening, Cation separations in electrodialysis through membranes coated with polyelectrolyte multilayers 55 (2014) 1397–1403, https://doi.org/10.1016/J.POLYMER.2013.12.002.
[15] T. Rijnaarts, D.M. Reurink, F. Radmanesh, W.M. de Vos, K. Nijmeijer, Layer-by-layer coatings on ion exchange membranes: effect of multilayer charge and hydration on monovalent ion selectivities, J. Membr. Sci. 570–571 (2019) 513–521, https://doi.org/10.1016/J.MEMSCI.2018.10.074.
[16] S. Chaudhury, A. Bhattacharyya, A. Goswami, Electrodriven ion transport through crown ether-nafion composite membrane: enhanced selectivity of Cs+ over Na+ by ion gating at the surface, Ind. Eng. Chem. Res. 53 (2014) 8804–8809, https://doi.org/10.1021/ie500934v.
[17] S. Yang, Y. Liu, J. Liao, H. Liu, Y. Jiang, B. Van Der Bruggen, J. Shen, C. Gao, Codeposition modification of cation exchange membranes with dopamine and crown ether to achieve high K+ electrodialysis selectivity, ACS Appl. Mater. Interfaces 11 (2019) 17730–17741, https://doi.org/10.1021/acsami.8b21031.
[18] L. Paltrinieri, E. Huerta, T. Puts, W. van Baak, A.B. Verver, E.J.R. Sudhölter, L.C.P. M. de Smet, Functionalized anion-exchange membranes facilitate electrodialysis of citrate and phosphate from model dairy wastewater, Environ. Sci. Technol. 53 (2018) 2396–2404, https://doi.org/10.1021/ACS.EST.8B05558.
[19] R. Epsztein, E. Shaulsky, M. Qin, M. Elimelech, Activation behavior for ion permeation in ion-exchange membranes: role of ion dehydration in selective transport, J. Membr. Sci. 580 (2019) 316–326, https://doi.org/10.1016/j.memsci.2019.02.009.
[20] Z. Qian, H. Miedema, S. Sahin, L.C.P.M. de Smet, E.J.R. Sudhölter, Separation of alkali metal cations by a supported liquid membrane (SLM) operating under electro dialysis (ED) conditions, Desalination 495 (2020), 114631, https://doi.org/10.1016/j.desal.2020.114631.
[21] M. Sadrzadeh, A. Razmi, T. Mohammadi, Separation of different ions from wastewater at various operating conditions using electrodialysis, Sep. Purif. Technol. 54 (2007) 147–156, https://doi.org/10.1016/j.seppur.2006.08.023.
[22] A.H. Galama, G. Daubaras, O.S. Burheim, H.H.M. Rijnaarts, J.W. Post, Seawater electrodialysis with preferential removal of divalent ions, J. Membr. Sci. 452 (2014) 219–228, https://doi.org/10.1016/j.memsci.2013.10.050.
[23] Y. Zhang, S. Paepen, L. Pinoy, B. Meesschaert, B. Van Der Bruggen, Selectrodialysis: fractionation of divalent ions from monovalent ions in a novel electrodialysis stack, Sep. Purif. Technol. 88 (2012) 191–201, https://doi.org/10.1016/j.seppur.2011.12.017.
[24] X.Y. Nie, S.Y. Sun, Z. Sun, X. Song, J.G. Yu, Ion-fractionation of lithium ions from magnesium ions by electrodialysis using monovalent selective ion-exchange membranes, Desalination 403 (2017) 128–135, https://doi.org/10.1016/j.desal.2016.05.010.
[25] M. Kumar, M.A. Khan, Z.A. AlOthman, M.R. Siddiqui, Polyaniline modified organic-inorganic hybrid cation-exchange membranes for the separation of

monovalent and multivalent ions, Desalination 325 (2013) 95–103, https://doi.org/10.1016/j.desal.2013.06.022.
[26] Y. Zhu, M. Ahmad, L. Yang, M. Misovich, A. Yaroshchuk, M.L. Bruening, Adsorption of polyelectrolyte multilayers imparts high monovalent/divalent cation selectivity to aliphatic polyamide cation-exchange membranes 537 (2017) 177–185, https://doi.org/10.1016/j.memsci.2017.05.043.
[27] T. Luo, S. Abdu, M. Wessling, Selectivity of ion exchange membranes: a review, J. Membr. Sci. 555 (2018) 429–454, https://doi.org/10.1016/j.memsci.2018.03.051.
[28] E.N. Durmaz, S. Sahin, E. Virga, S. de Beer, L.C.P.M. de Smet, W.M. de Vos, Polyelectrolytes as building blocks for next-generation membranes with advanced functionalities, ACS Appl. Polym. Mater. 3 (2021) 4347–4374, https://doi.org/10.1021/ACSAPM.1C00654.
[29] Z. Qian, H. Miedema, L.C.P.M. de Smet, E.J.R. Sudhölter, Modelling the selective removal of sodium ions from greenhouse irrigation water using membrane technology, Chem. Eng. Res. Des. 134 (2018) 154–161, https://doi.org/10.1016/j.cherd.2018.03.040.
[30] N.M. Kocherginsky, Q. Yang, L. Seelam, Recent advances in supported liquid membrane technology, Sep. Purif. Technol. 53 (2007) 171–177, https://doi.org/10.1016/j.seppur.2006.06.022.
[31] P.K. Parhi, Supported liquid membrane principle and its practices: a short review, J. Chem. 2013 (2013) 1–11, https://doi.org/10.1155/2013/618236.
[32] E. Bakker, E. Pretsch, Lipophilicity of tetraphenylborate derivatives as anionic sites in neutral carrier-based solvent polymeric membranes and lifetime of corresponding ion-selective electrochemical and optical sensors, Anal. Chim. Acta 309 (1995) 7–17, https://doi.org/10.1016/0003-2670(95)00077-D.
[33] T. Rosatzin, E. Bakker, K. Suzuki, W. Simon, Lipophilic and immobilized anionic additives in solvent polymeric membranes of cation-selective chemical sensors, Anal. Chim. Acta 280 (1993) 197–208, https://doi.org/10.1016/0003-2670(93)85122-Z.
[34] F.G. Bănică, John Wiley and Sons, ChichesterUK, 2012, https://doi.org/10.1002/9781118354162.
[35] H. Kreulen, C.A. Smolders, G.F. Versteeg, W.P.M. Van Swaaij, Determination of mass transfer rates in wetted and non-wetted microporous membranes, Chem. Eng. Sci. 48 (1993) 2093–2102, https://doi.org/10.1016/0009-2509(93)80084-4.
[36] M. Khayet, J.I. Mengual, G. Zakrzewska-Trznadel, Direct contact membrane distillation for nuclear desalination. Part I: review of membranes used in membrane distillation and methods for their characterisation, 2005.
[37] Y. Tanaka, 2nd ed., Elsevier, 2015. https://www.elsevier.com/books/ion-exchange-membranes/tanaka/978-0-444-63319-4.
[38] J.M. Zook, J. Langmaier, E. Lindner, Current-polarized ion-selective membranes: the influence of plasticizer and lipophilic background electrolyte on concentration profiles, resistance, and voltage transients, Sensors Actuators B Chem. 136 (2009) 410–418, https://doi.org/10.1016/j.snb.2008.12.047.
[39] A. Kumar, P.S.H. Rizvi, A.M.S. Requena, Handbook of Membrane Separations: Chemical, Pharmaceutical, Food, and Biotechnological Applications, 2nd ed., CRC Press, 2015.
[40] Peter Atkins, Julio de Paula, James Keeler, Atkins' Physical Chemistry, Oxford University Press, 2006.
[41] M. Born, Volumen und Hydratationswärme der ionen 1 (1920) 45–48, https://doi.org/10.1007/BF01881023.
[42] E.R. Nightingale, Phenomenological theory of ion solvation. Effective radii of hydrated ions, J. Phys. Chem. 63 (1959) 1381–1387, https://doi.org/10.1021/j150579a011.
[43] R.A. Robinson, R.H. Stokes, SecondRevised Edition, 2002.
[44] L. Lizana, A.Y. Grosberg, Exact expressions for the mobility and electrophoretic mobility of a weakly charged sphere in a simple electrolyte, 2014.
[45] Z. Samec, J. Langmaier, A. Trojánek, E. Samcová, J.Í. Málek, J. Heyrovskýinstituteheyrovský, Transfer of protonated anesthetics across the water|o-nitrophenyl octyl ether interface: effect of the ion structure on the transfer kinetics and pharmacological activity, 1998.